OSR
ORAL SCIENCES REPORTS

Original Article


***Editor:***
Papimon Chompu-Inwai,
Chiang Mai University, Thailand

*Received: April 30, 2024*
*Revised: June 20, 2024*
*Accepted: July 31, 2024*

***Corresponding Author:***
Asst. Prof. Dr. Sitthikorn Kunawarote,
Department of Restorative Dentistry and Periodontology, Faculty of Dentistry, Chiang Mai University, Chiang Mai 50200, Thailand.
E-mail: sitthikorn.k@cmu.ac.th

Oral Sci Rep. 2024; 45(2): 49-61

# Remineralization Potential of Nano-strontium/Fluoride Hydroxyapatite on Artificial Enamel Caries

*Natcha Boontanapibul[1], Sitthikorn Kunawarote[2]*

*[1]Master's Student, Master of Science Program in Dentistry, Department of Restorative Dentistry and Periodontology, Faculty of Dentistry, Chiang Mai University, Thailand*
*[2]Department of Restorative Dentistry and Periodontology, Faculty of Dentistry, Chiang Mai University, Thailand*

## Abstract

**Objectives:** This study aimed to evaluate the remineralization efficacy of nano-strontium/fluoride hydroxyapatite paste on initial enamel caries in comparison with other remineralization products under a simulated pH-cycling model.

**Methods:** Following the artificial caries induction, forty enamel specimens with non-cavitated lesion in the same range of lesion depth were selected by mean of micro-CT evaluation. The specimens were block-randomized into four experimental groups regarding remineralizing pastes: 1500 ppm sodium fluoride paste, 10%wt nano-hydroxyapatite paste, 10%wt nano-strontium/fluoride hydroxyapatite paste and 5%wt nano-strontium/fluoride hydroxyapatite paste. Remineralizing effect was evaluated using micro-CT, while SEM/EDS line scan mode facilitated the investigation of remineralization patterns. Changes in lesion depth (ΔLD) and changes in mineral loss (ΔΔZ) were evaluated at 7 and 14 days of treatment under the pH-cycling model. Statistical analyses were performed using 2-way ANOVA and post hoc Tukey's test ($p<0.05$).

**Results:** The use of 5%wt nano-strontium/fluoride hydroxyapatite paste significantly reduced lesion depth in initial caries under experimental conditions. Meanwhile, the 10%wt nano-strontium/fluoride hydroxyapatite paste yielded the highest mineral gain, though statistically insignificant. EDS graphs indicated an increasing calcium and phosphorus deposition trend over time with nano-strontium/fluoride hydroxyapatite paste, revealing a more uniform mineral distribution compared to both sodium fluoride and nano-hydroxyapatite pastes. Nevertheless, neither fluorine nor strontium was detectable in these graphs.

**Conclusions:** The study revealed comparable remineralization efficacy with 5%wt and 10%wt nano-strontium/fluoride hydroxyapatite pastes. The treatment durations of 7 and 14 days showed no significant difference in outcomes.

**Keywords:** initial caries, lesion depth, mineral gain, nano-strontium/fluoride hydroxyapatite, remineralization

## Introduction

Dental caries is the outcome of an imbalance between remineralization and demineralization processes. This widespread disease is caused by acid-producing bacteria that ferment carbohydrates. The first sign of dental caries is enamel caries or white spot lesion. The white spot lesion has an intact enamel surface and is reversible as this non-cavitated lesion is caused by subsurface demineralization.[1,2] The movement of calcium and phosphate ions from dissolving enamel, in conjunction with fluoride ions from the oral environment, enhance the acid resistance of enamel surface. As a result, demineralization predominantly affects the subsurface region rather than the superficial enamel.[2] The continuous process of mineral loss led to the structural breakdown of the tooth surface or cavitated carious lesion. This process can be arrested through dietary modifications that balance the acid-base level, and sufficient cleaning with a therapeutic agent.[1] Minimal intervention dentistry is the concept of preserving the tooth structure and preventing further carious experiences.[3] The therapeutic intervention with remineralizing agents enhance remineralization and inhibit the demineralization process.[4] Remineralization of enamel occurs when the concentration of calcium and phosphate ions in saliva and biofilm is supersaturated compared to those of the enamel. This process leads to the inhibition of further mineral loss and the repair of the partially demineralized hydroxyapatite of the enamel.[5,6] Remineralizing agents have been widely classified into fluorides and non-fluoride remineralizing agents.[7] The most common among them is fluoride, typically at concentrations between 1000-1500 ppm.[3,8] There are many fluoride-containing products on the market including toothpaste, mouth rinses, and pastes.

Fluoride is a multifaceted agent against dental caries, functioning through three primary mechanisms, inhibiting demineralization, enhancement of remineralization, and antimicrobial actions.[1,2] After acidic exposures, saliva neutralizes the acids. When the pH surpasses 5.5, the natural remineralization takes place. In this environment, fluoride in the saliva plays a pivotal role in expediting the remineralization process.[1] Fluoride ions adsorbing to the surface of partially demineralized crystals, subsequently attracting calcium ions.[1,9,10] This leads to the formation of modified enamel crystal, fluorapatite, which enhance the enamels resistance to the further acidic challenges.[1,10,11] Additionally, fluoride in the form of hydrogen fluoride infiltrates bacterial cells, it disrupts bacterial glycolytic enzymes, leading to diminished acid production[1,12] and reduced bacterial adherence to teeth.[1,13] However, it is imperative to supervise fluoride consumption in children up to 6 years old as excessive consumption through mouth rinses or toothpaste can lead to acute or chronic fluoride toxicity.[1,13,14]

Non-fluoride remineralizing agents and biomimetic approaches have become outstanding since they have the potential to remineralize teeth using biomaterials such as nano-hydroxyapatite. Recent research has focused on nanohydroxyapatite due to its remarkable similarity to the hydroxyapatite crystals found in enamel, encompassing size, crystal structure, and chemical composition.[15,16] These characteristics confer biocompatibility, referring to the ability of a material to perform with an appropriate host response in a specific situation, and bioactivity, indicating the ability to induce favorable biological interactions.[15] Previous studies confirmed that nano-hydroxyapatite effectively remineralized the initial caries.[4,17-23] Nanohydroxyapatite's mechanism of action includes filling the micropores of demineralized enamel[20], thus forming an apatite-layer over the enamel surface.[21,22] Moreover, nano-hydroxyapatite serves as a reservoir of calcium and phosphate ions, facilitating the remineralization of demineralized enamel.[19] Although nano-hydroxyapatite is associated with a high degree of crystallinity, which tends to increase with concentration, research indicates that the optimum concentration is 10% by weight.[23]

Ionic substitutions of calcium in nano-hydroxyapatite lead to modifications of the physicochemical properties.[24-26] Specifically, strontium substitution induces crystal asymmetry, increases solubility but reduces crystallinity. In contrast, fluoride substitution leads to crystal lattice contraction, enhancing both stability and crystallinity of the nanoparticle. The combined inclusion of strontium and fluoride in nano-strontium/fluoride hydroxyapatite causes slightly distortion and a smaller crystal lattice, resulting in lower solubility compared to both pure nano-hydroxyapatite and nano-strontium hydroxyapatite. Moreover, nano-strontium/fluoride hydroxyapatite also exhibits less crystallinity compared to pure nano-hydroxyapatite. Furthermore, studies suggest that ion-substituted hydroxyapatite exhibited lower

cytotoxicity than pure nano-hydroxyapatite.[26,27]

This study aimed to assess the remineralization efficacy of various remineralizing pastes and to explore the patterns of remineralization under a pH-cycling model. Specifically, the experiment focuses on the comparison of a nano-strontium/fluoride hydroxyapatite paste with a 1500 ppm fluoride paste and a 10%wt nano-hydroxyapatite paste. The hydrothermal synthesis, involving the substitution of strontium and fluoride ions into nano-hydroxyapatite, yields rod-shaped nano-strontium/fluoride hydroxyapatite crystals ranging between 20 to 60 nm. As nano-strontium/fluoride hydroxyapatite exhibits physicochemical properties more prone to remineralization, it is more stable and exhibits less crystallinity compared to nano-hydroxyapatite.[26,27] While nano-hydroxyapatite crystallinity increases with concentration.[23] The concentrations of 5% and 10% nano-strontium/fluoride hydroxyapatite were tested to determine the optimal concentration. Remarkably, as per our knowledge, no previous research has compared these specific pastes using both micro-CT and SEM/EDS analytical techniques. This novel approach promises not only to deepen the understanding of remineralization strategies, but also to pave the way for new avenues in research and potential advancements in dental health practices.

## Materials and Methods

### *Preparation of enamel specimens*

Sixty human permanent premolar teeth were extracted due to orthodontic treatment or periodontal disease with the intact crown and no developmental lesion. The study received ethical approval from the Human Experimental Committee of the Faculty of Dentistry at Chiang Mai University, Chiang Mai, Thailand (No. 1/2022). The teeth were cleaned by ultrasonic scaler and stored in 0.1% thymol solution. Sixty cubic specimens, each measuring 4x4x4 (width x length x thickness) cubic millimeters were obtained from the buccal portion of the teeth and subsequently embedded in blocks of acrylic resin. The enamel surface was polished using a grinding/polishing machine (Mopao 160E, LaiZhou Weiyi Experimental Machinery Manufacture, Shandong, China) with silicon-carbide sandpapers at 600-, 1000-, 1500-, and 2000-grit, respectively, with water for 1 minute per each roughness. This process was performed to align the flat enamel surface with the acrylic resin block surface. Post-polishing, all specimens were cleaned using an ultrasonic cleanser (BioSonic UC125, Whaledent Inc, OH, USA) for 10 minutes.

### *Artificial initial caries formation*

Each enamel specimen was divided into three parts, each approximately 1 mm width. The central segment was coated with clear nail varnish to preserve as a sound enamel control. The left and right segments were kept uncoated, serving as the demineralized enamel control and the section undergoing pH-cycling treatment. Following the preparation, specimens were immersed in 5 ml of acetic acid buffer solution with a pH of 4.5 and a temperature of 37°C for a period of seven days as shown in Table 1. In the preparation of the specimens, the method was modified from Vacharangkura A, and Kunawarote S, as detailed in the the proceedings of 6$^{th}$ RSU International

**Table 1:** The composition of solutions in the experiment

| Solutions | Compositions | pH and Temperature |
|---|---|---|
| Acetic acid buffer solution | 50 mM acetic acid<br>2.2 mM calcium chloride ($CaCl_2$•$2H_2O$)<br>2.2 mM potassium dihydrogen phosphate ($KH_2PO_4$)<br>0.1 ppm of fluoride | pH 4.5<br>37°C |
| Remineralized solution | 130 mM potassium chloride (KCl)<br>1.5 mM calcium chloride ($CaCl_2$•$2H_2O$)<br>0.9 mM of potassium dihydrogen phosphate ($KH_2PO_4$)<br>20 mM of HEPES buffer | pH 7.0<br>37°C |
| Demineralized solution | 50 mM of acetic acid<br>2.2 mM calcium chloride ($CaCl_2$•$2H_2O$)<br>2.2 mM potassium dihydrogen phosphate ($KH_2PO_4$) | pH 4.5<br>37°C |

Research Conference on Science and Technology (2021), illustrated in Figure 1.[28]

After the formation of artificial initial caries, the specimens were sectioned to obtain a slice of 1 mm thickness cross-sectioned specimen from each specimen using a low-speed precision cutting machine (IsoMet™, BUEHLER, Illinois, USA). Initial evaluations were conducted using micro-CT (microCT35, SCANCO Medical AG, Brüttisellen, Switzerland) to analyze mineral density, which was then used to determine the lesion depth (LD) and mineral loss (ΔZ). Furthermore, the elemental composition and remineralization pattern were examined using the Scanning Electron Microscope and Energy Dispersive X-ray Analysis Systems (SEM/EDS) (Quanta250, FEI company, Oregon, USA) operated in line scan mode.

### *Remineralizing treatment*

After assessment of the artificial initial caries lesions using micro-CT, forty enamel specimens with non-cavitated enamel lesion, and a normalized mean lesion depth were selected. The normalization achieved by excluding the top and bottom deciles of the distribution. To maintain the integrity of the specimens, both the cut surfaces and the demineralized sections were coated with nail varnish. Subsequently, the specimens were systematically allocated into four experimental groups via block-randomization, regarding remineralizing pastes: 1500 ppm sodium fluoride paste (F), 10%wt nano-hydroxyapatite paste (nHA), 10%wt nano-strontium/fluoride hydroxyapatite paste (SrF10), and 5%wt nano-strontium/fluoride hydroxyapatite paste (SrF5), which is rod-shaped, measuring 20-60 nm in length and 10 nm in diameter. The molecular formula of nano-strontium/fluoride hydroxyapatite within the pastes is $Sr_5Ca_5(PO_4)_6F_2$. Within each group, specimens were randomly selected to represent the full range of EDS patterns of that specific group.

For each group, the specimens received identical paste application procedures. A 0.05 ml of the respective paste, with its composition provided in Table 2, was applied onto the moist enamel, emulating oral cavity conditions. The paste was then left on the specimen for five minutes, simulating the effect of paste retention on teeth during periods of non-consumption. Thereafter, the specimens were immersed in remineralizing solutions for an additional 25 minutes. Finally, after a total of 30 minutes of remineralizing paste application, each specimen was thoroughly rinsed with distilled deionized water before being subjected to simulated pH-cycling.

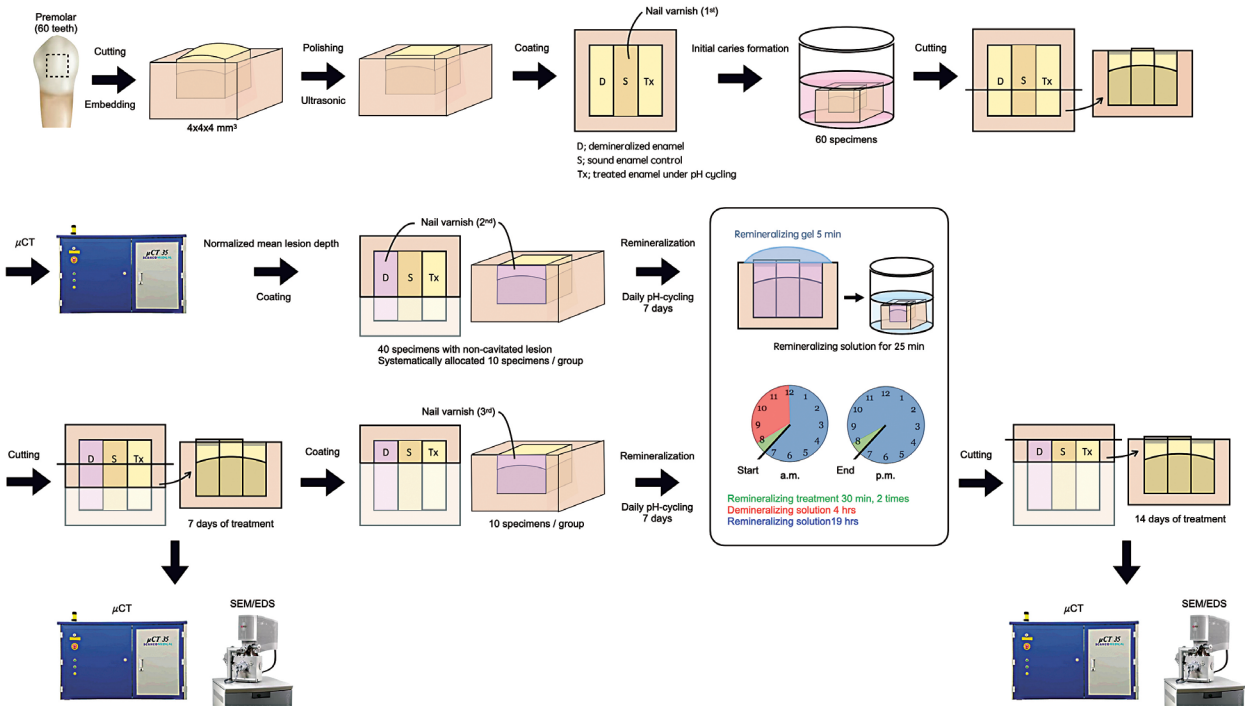


**Figure 1:** Experimental procedures for specimen preparation and remineralization assessment. The figure illustrates the steps involved in specimen preparation and measurements, including remineralization assessments at 7 days and 14 days using micro-CT and scanning electron microscope and energy dispersive x-ray analysis system (SEM/EDS)

### *Micro-CT*

The cross-sectioned specimens were mounted perpendicularly to the x-ray beam, which was set to 70kV and 114 µA. The scans resulted in 8-bit grayscale TIFF format images, each having a resolution of 1,024 x 1,024 pixels and a voxel size of 5 µm. These images were analyzed using the ImageJ software (NIH, Bethesda, MD, USA). Using the enamel surface as a starting point, the grayscale values were converted to mineral densities for comparison with the sound enamel control. The variables included mineral density profiles, with $MD_B$ representing baseline mineral density and $MD_D$ representing demineralized mineral density. These profiles were used to calculate lesion depth ($LD_D$ as demineralized lesion depth) and mineral loss ($\Delta Z_D$ as mineral loss after demineralization). Lesion depth was determined based on the depth of the mineral volume at 95% of the maximum mineral density, and mineral loss was calculated from the area under the graph, which compared the mineral densities of sound and demineralized enamel.[29]

### *SEM/EDS*

The cross-sectioned specimens were desiccated using silica gel to remove moisture prior to examination with the SEM/EDS. The specimens were mounted on the sample holder of the scanning electron microscope (Quanta 250, FEI company, Oregon, USA) for cross-sectional elemental analysis. The settings were adjusted to 20 kV, with a magnification of 500 times. The elemental analysis program (Aztec, Oxford Instruments plc, Abingdon, UK) was used in line scan mode. The origin of the depth axis was referenced from the visible surface of the enamel specimen. The program then processed the elemental intensities and generated a graph showing the relationship

**Table 2:** The compositions of remineralizing pastes (%wt)

| | F | nHA | SrF10 | SrF5 |
|---|---|---|---|---|
| Deionized water | 58.92 | 49.25 | 49.25 | 54.25 |
| Sorbitol | 30.00 | 30.00 | 30.00 | 30.00 |
| Thickening silica | 8.00 | 8.00 | 8.00 | 8.00 |
| Carboxymethyl cellulose | 1.50 | 1.50 | 1.50 | 1.50 |
| Flavor | 0.80 | 0.80 | 0.80 | 0.80 |
| Titanium dioxide | 0.20 | 0.20 | 0.20 | 0.20 |
| Sodium benzoate | 0.25 | 0.25 | 0.25 | 0.25 |
| Sodium fluoride | 0.33 | - | - | - |
| n-HA | - | 10.00 | - | - |
| n-Sr/F HA | - | - | 10.00 | 5.00 |
| Total | 100.00 | 100.00 | 100.00 | 100.00 |

*n-HA, 10%wt nano-hydroxyapatite paste SrF10; 10%wt nano-strontium/fluoride hydroxyapatite paste; SrF5, 5%wt nano-strontium/fluoride hydroxyapatite paste*

**Table 3:** The variables in this study

| Variables | Sound enamel | After demineralization | After Treatment 7 days | Changes in 7 days | After Treatment 14 days | Changes in 14 days |
|---|---|---|---|---|---|---|
| Lesion depth (LD) | - | $LD_D$ | $LD_1$ | $\Delta LD_1$ ($LD_1$ - $LD_D$) | $LD_2$ | $\Delta LD_2$ ($LD_2$ - $LD_D$) |
| Mineral loss ($\Delta Z$) | Control ($MD_B$) | $\Delta Z_D$ ($MD_D$ - $MD_B$) | $\Delta Z_1$ ($MD_7$ - $MD_B$) | $\Delta\Delta Z_1$ ($\Delta Z_1$ - $\Delta Z_D$) | $\Delta Z_2$ ($MD_{14}$ - $MD_B$) | $\Delta\Delta Z_2$ ($\Delta Z_2$ - $\Delta Z_D$) |

*$LD_D$ is lesion depth after demineralization*
*$MD_B$ is mineral density of the sound enamel*
*$MD_D$ is mineral density after demineralization*
*$MD_7$ is mineral density at 7 days of remineralized treatment*
*$MD_{14}$ is mineral density at 14 days of remineralized treatment*

between the X-ray signal in counts per second (cps) and the measurement distance in μm.

### *Simulated pH-cycling*

To replicate the natural oral environment, a pH-cycling routine was employed, involving a 19-hour immersion of specimens in a remineralization solution and a 4-hour exposure to an acetic buffer solution with pH 4.5[30] for demineralization, as described in Table 1. The remineralizing pastes were applied twice daily in 30-minute durations: once before the demineralization period, and a second time 12 hours later. The solutions were refreshed daily. Assessments of the remineralization process were then conducted on the 7$^{th}$ and 14$^{th}$ days of the cycle.

### *Remineralization assessments*

After 7 and 14 days of remineralizing treatment along with pH-cycling, the enamel specimens were sectioned into 1 mm thickness. The cross-sectional enamel specimens were evaluated using micro-CT and SEM/EDS. The data of mineral density were gathered at 7 days ($MD_7$) and 14 days ($MD_{14}$). The calculation was performed in the term of lesion depth ($LD_1$ and $LD_2$) and mineral loss ($\Delta Z_1$ and $\Delta Z_2$). The SEM/EDS concentrated on elemental composition and remineralization patterns across the different groups of enamel specimens treated with various pastes. The assessments were conducted across four stages: sound enamel control, demineralized enamel, 7 days of treatment, and 14 days of treatment. The EDS graphs provides an overview of mineral changes across stages, enhancing the understanding of the remineralization process.

### *Statistical analysis*

The changes in lesion depth ($\Delta LD_1$ and $\Delta LD_2$) and the changes of mineral loss ($\Delta\Delta Z_1$ and $\Delta\Delta Z_2$) were quantitatively analyzed as presented in the Table 3. The data was subjected to statistical analysis using statistics software (SPSS version 28.0, IBM Corporation, Armonk, NY, USA). Normal distribution of the data was evaluated using the Shapiro-Wilk test, while variance homogeneity was analyzed using the Levene statistic. Changes in mineral loss ($\Delta\Delta Z$) and lesion depth ($\Delta LD$) after treatment for 7 and 14 days of treatment across the experimental groups were analyzed using two-way ANOVA, followed by post hoc Tukey's significant difference test. All statistical analyses were performed at a 95% confidence interval with 80% power of the test.

## Results

Forty specimens with non cavitated lesion were selected after the formation of artificially demineralized enamel, based on the mean lesion depth. The mean lesion depth after demineralization ($LD_D$) was 151.2±24.4 μm. The specimens were block randomized into four groups. After the pH-cycling model treatment, the mean changes in lesion depth and mineral loss were evaluated, as shown in Table 4.

Micro-CT imaging in Figure 2 revealed increased radiolucency in demineralized enamel, whereas the outermost layer maintained consistency with normal enamel. The images of the specimens after demineralization displayed enhanced radiopacity. The fluoride paste-treated group exhibited a reduction in the depth of the radiolucent layer and an increase in surface radiopacity. Conversely, groups treated with nHA, SrF10 and SrF5 showed a reduction in the depth of the radiolucent layer and an increase in radiopacity throughout the lesion.

**Table 4:** The mean and standard deviations of the change in lesion depth (μm) and the change in mineral loss (mgHAP/m$^2$) of the experimental groups under the simulated pH-cycling model at different timing

| Experimental groups | Change in lesion depth on day 7 ($\Delta LD_1$) | Change in lesion depth on day 14 ($\Delta LD_2$) | Change in mineral loss on day 7 ($\Delta\Delta Z_1$) | Change in mineral loss on day 14 ($\Delta\Delta Z_2$) |
|---|---|---|---|---|
| F group | 10.6 (35.3)$^{a}$ | -1.2 (31.9) | -466.6 (9484.3) | -768.5 (11340.5) |
| nHA group | 10.6 (37.9)$^{a}$ | 2.0 (32.5) | -35.4 (13735.7) | -363.6 (7760.1) |
| SrF10 group | -13.9 (39.1)$^{ab}$ | -18.6 (32.6) | -5744.9 (9288.1) | -6534.3 (10880.3) |
| SrF5 group | -19.0 (25.0)$^{b}$ | -26.8 (21.9) | -4877.8 (5100.0) | -3553.1 (6271.0) |

*Alphabets that are labeled with a different letter indicate significant differences within the same period across varying treatments ($p<0.05$)*

### *Lesion depth*

In the comparison of mean changes in lesion depth between the experimental groups over the period of 7 and 14 days, it was found that the experimental groups showed distinct changes in lesion depth. At 7 days, the SrF5 group showed significantly reduced lesion depth compared with other groups, with the exception of the SrF10 group. This was followed by the fluoride paste group, and the nHA group. Furthermore, all groups demonstrated decreased lesion depths corresponding trends of remineralization at 14 days with no statistically significant difference as shown in Table 4.

### *Mineral loss*

The mean changes in mineral loss between the experimental groups and periods were shown in Table 4. The alteration in negative value indicated the mineral deposition or remineralization on the demineralized enamel. The mean of change in the mineral loss of the SrF10 group demonstrated the most negative values, followed by SrF5 group, and nHA group. Over the usage period, the SrF10 group exhibited the most mineral deposition. However, the data revealed no statistical difference among experimental groups and no difference between the 7 and 14-day periods.

### *Remineralizing patterns*

The SEM/EDS method provided patterns of elemental intensity as qualitative data. The cross-sectional surfaces of sound enamel, demineralized enamel and treated enamel were evaluated. For each experimental group, one specimen was randomly selected to represent the EDS pattern. Following artificial demineralization, the graphs showing the intensity of calcium (Ca) and phosphorus (P) elements demonstrated less uniformity compared to sound enamel. However, after 7 and 14 days of the remineralizing treatment under the pH-cycling model, notable changes in the EDS graphs were observed. The group treated with fluoride paste exhibited an increase in Ca and P elemental intensity compared to demineralized enamel. By the 14$^{th}$ day, the EDS graph reflected intensity levels approximating those of the sound enamel control, though the mineral deposition was disorganized and non-uniform. Notably, an increase in intensity was also observed at the surface. Meanwhile, the groups treated with nHA, SrF10 and SrF5 showed increased Ca and P intensity along the depth of lesion. By the 14$^{th}$ day of treatment, the EDS graphs revealed intensities akin to the sound enamel control, displaying homogeneity in mineral deposition and uniform distribution. Nonetheless, strontium and fluorine were barely detected in the EDS, as shown in Figure 3-6.

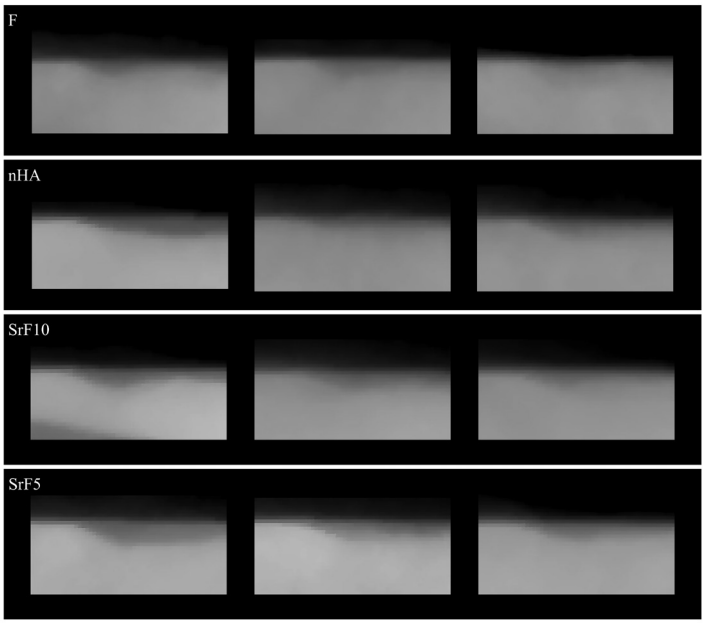


**Figure 2:** Micro-CT images illustrating the progression of the radiolucency areas in experimental groups. From left to right: artificially demineralized enamel, specimens treated with remineralizing paste under simulated pH-cycling for 7 days, and specimens after 14 days of treatment

**SrF10 group**

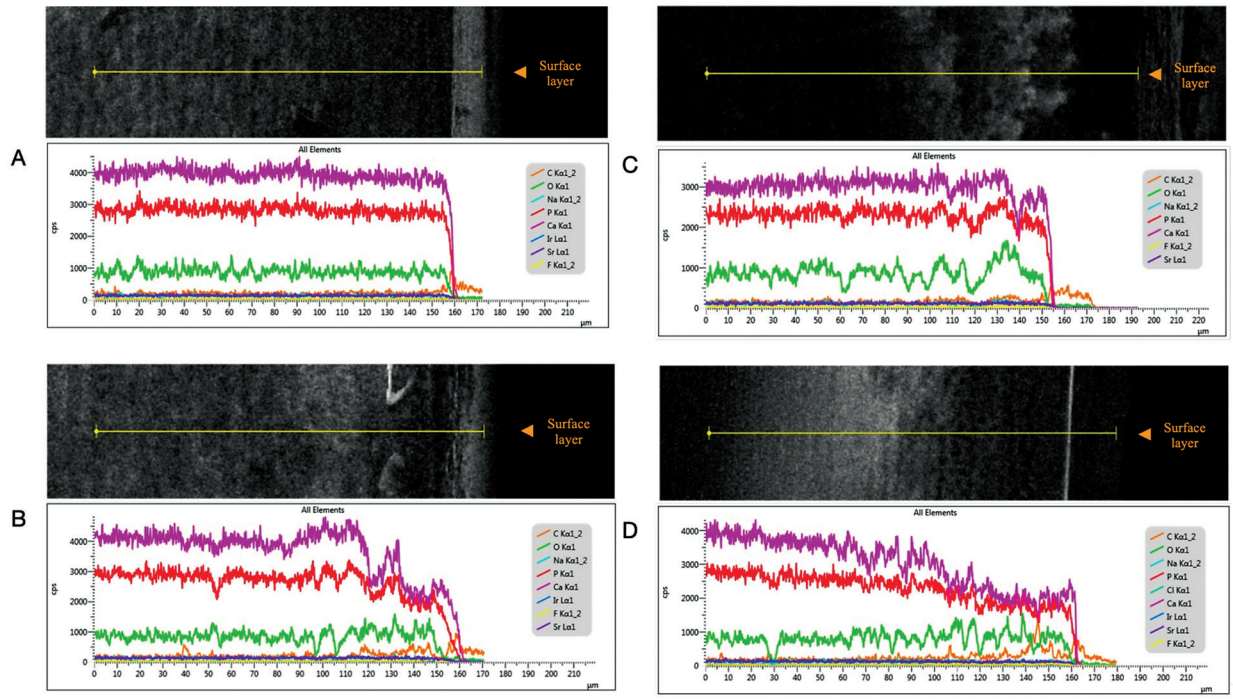


**Figure 3:** Energy dispersive x-ray analysis systems (EDS) line graphs and images represent element intensity in various enamel conditions, sound enamel control (A), demineralized enamel (B), treated with 1500 ppm sodium fluoride paste under simulated pH-cycling for 7 days (C), and treated with 1500 ppm sodium fluoride paste under simulated pH-cycling for 14 days (D)

**SrF5 group**

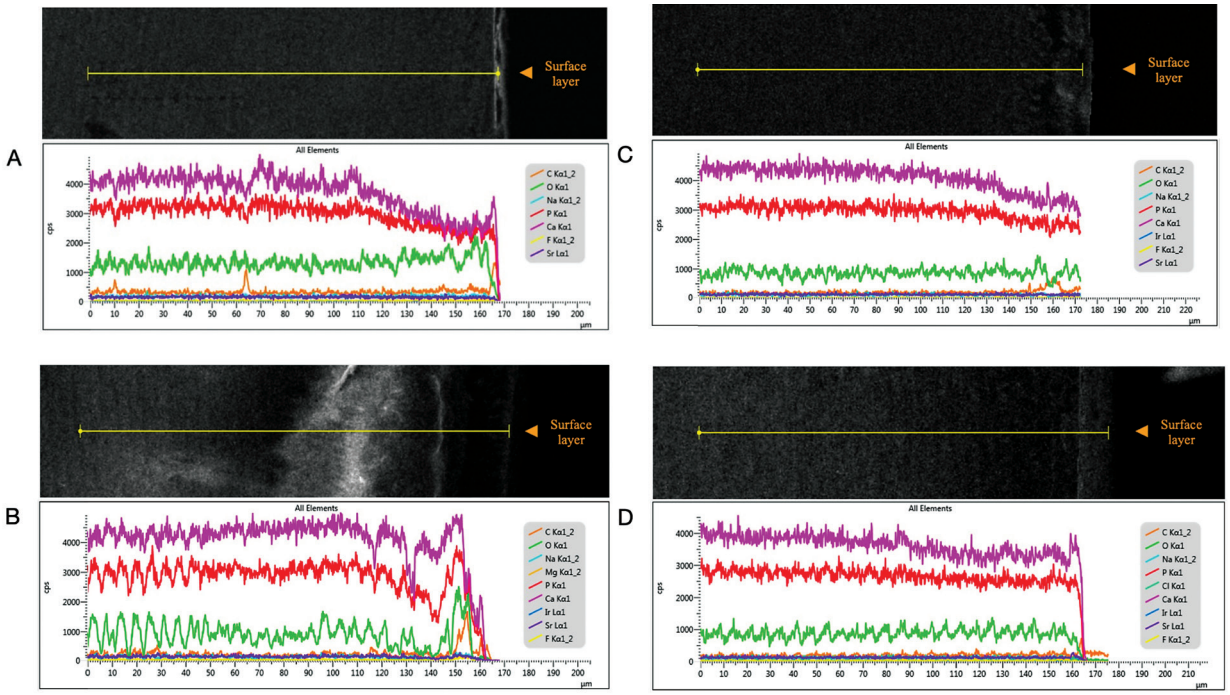


**Figure 4:** Energy dispersive x-ray analysis systems (EDS) line graphs and images represent element intensity in various enamel conditions, sound enamel control (A), demineralized enamel (B), treated with 10%wt nano-hydroxyapatite paste under simulated pH-cycling for 7 days (C), and treated with 10%wt nano-hydroxyapatite paste under simulated pH-cycling for 14 days (D)

**SrF10 group**

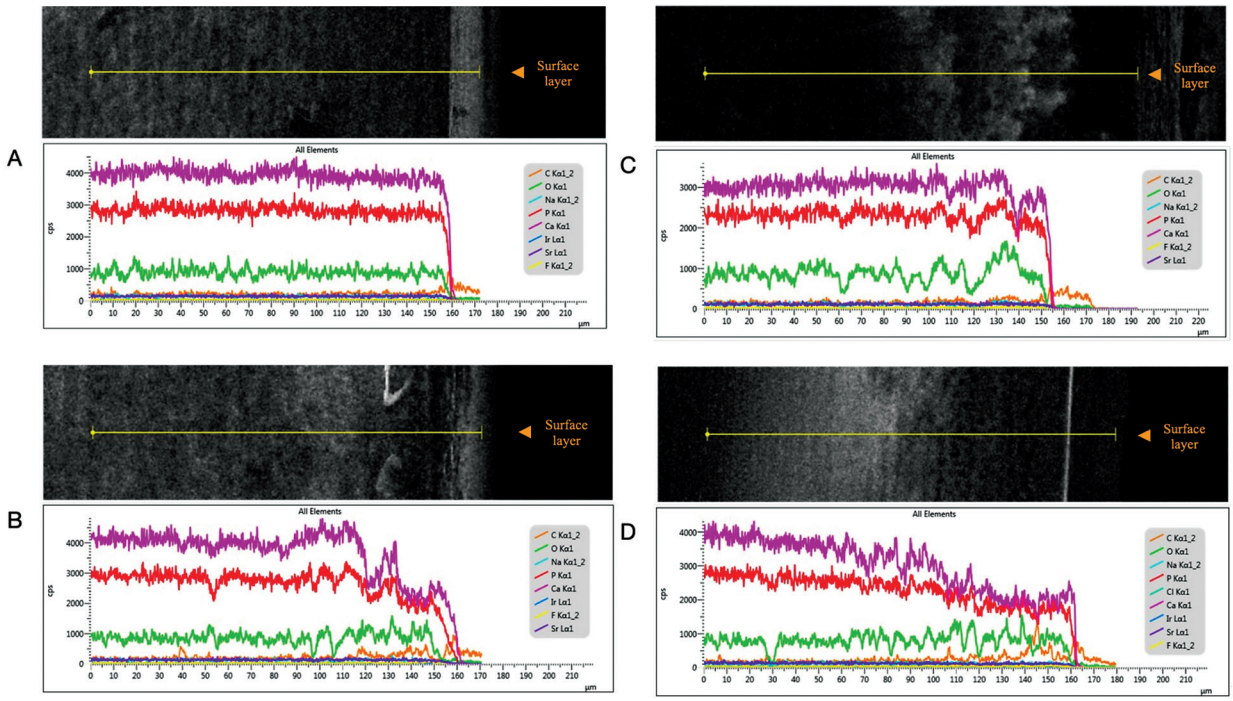


**Figure 5:** Energy dispersive x-ray analysis systems (EDS) line graphs and images represent element intensity in various enamel conditions, sound enamel control (A), demineralized enamel (B), treated with 10%wt nano-strontium/fluoride hydroxyapatite paste under simulated pH-cycling for 7 days (C), and treated with 10%wt nano-strontium/fluoride hydroxyapatite paste under simulated pH-cycling for 14 days (D)

**SrF5 group**

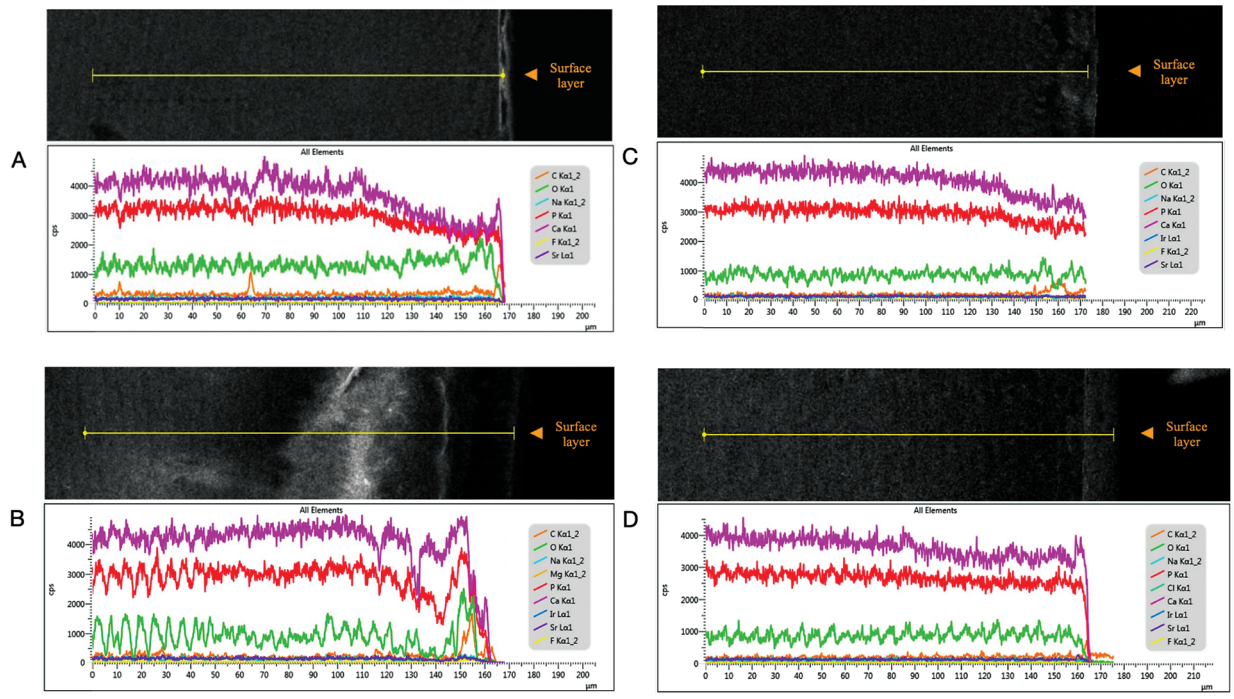


**Figure 6:** Energy dispersive x-ray analysis systems (EDS) line graphs and images represent element intensity in various enamel conditions, sound enamel control (A), demineralized enamel (B), treated with 5%wt nano-strontium/fluoride hydroxyapatite paste under simulated pH-cycling for 7 days (C), and treated with 5%wt nano-strontium/fluoride hydroxyapatite paste under simulated pH-cycling for 14 days (D)

## Discussion

In establishing the experimental design for this study, lesion depth was selected as the baseline parameter to standardize initial lesion severity across all specimens. This ensured that any observed effects could be attributed to the remineralizing pastes being tested. Specimens were then randomized into four groups using block-randomization to maintain balance in group allocation. Although this approach may have introduced variability in initial mineral loss or mineral density among the groups, our analysis confirmed that the distribution of both lesion depth and mineral density remained normally distributed. This is pivotal, as the lesion depth parameter was derived from the calculation of mineral loss, comparing mineral density to that of sound enamel controls. This methodological framework provides a robust basis for the observed significant reductions in lesion depth and indications of mineral loss when using nano-strontium/fluoride hydroxyapatite, underscoring its potential as a viable alternative to traditional fluoride treatments in managing initial enamel caries.

Early demineralized enamel caries or initial enamel caries can be treated with non-invasive treatments such as remineralizing agents. Fluoride with a concentration of 1500 ppm is recognized as an effective remineralizing agent on initial enamel caries. However, recent studies indicate that nano-hydroxyapatite could be a compelling alternative. Nanotechnology biomaterials, especially nano-hydroxyapatite, have gained attention due to their enhanced bioactivity and biocompatibility properties. In our study, the hydrothermal synthesis combined with the strontium and fluoride ions substitution yields rod-shaped nano-strontium/fluoride hydroxyapatite crystals ranging between 20 to 60 nm. This specific morphology is not only safer when compared to other shapes of nano-hydroxyapatite[31], but it also exhibited significantly greater remineralization, along with a significant reduction in both lesion depth and mineral loss, when compared to sodium fluoride and standard nano-hydroxyapatite.

The rod-like shape of the nano-strontium/fluoride hydroxyapatite crystals may play a crucial role in their efficacy for caries prevention. Our data suggest that strontium/fluoride doping not only modifies the shape of nano-hydroxyapatite but also significantly improves its remineralization potential, leading to increased mineral density and reduced lesion depth compared to conventional nano-hydroxyapatite. This indicates that the rod-shaped structure could better facilitate penetration into the micropores of enamel, thereby potentially improving caries prevention. According to previous research, rod-shaped crystals have been found to be less detrimental to rat aortic smooth muscle cells compared to other shapes of nano-hydroxyapatite[31], highlighting their promising safety characteristics for dental applications. Such morphological properties of the crystals are essential when considering their integration with dental enamel and the necessity for minimal tissue-related side effects. Despite promising preliminary evidence, the comprehensive biological implications of these crystals need to be understood better through extensive further studies.

The mechanism under acidic conditions, these rod-shaped nano-strontium/fluoride hydroxyapatite crystals dissolve, releasing strontium, fluoride, calcium, and phosphate ions. These released ions are critical for the remineralization process. The released ions contribute to the remineralization of demineralized enamel, replenishing lost minerals and thus helping to restore the structural integrity and strength of the enamel. Further studies are required to explore the possibility of these ions counteracting the acidification caused by cariogenic bacteria in the oral environment.

In the current study, nano-strontium/fluoride hydroxyapatite pastes exhibit a significant remineralization efficacy on initial caries under experimental conditions. Due to the ions-substitution up to 50 mol% strontium induces lattice distortion and decreases crystal symmetry. In contrast, fluoride substitution causes the lattice contraction and enhances crystallinity. However, the co-doped strontium/fluoride substitution causes slight distortion and smaller lattice parameters. Consequently, the nano-strontium/fluoride hydroxyapatite proves more stable than strontium-substitution hydroxyapatite but displays less crystallinity than fluoride-substitution hydroxyapatite and pure hydroxyapatite.[26,27] The co-doped strontium/fluoride substitution, combined with hydrothermal synthesis, produces nanometer-sized crystals. These modifications increased stability[27], promoting micropore filling, and reduce crystallinity[27], thereby preventing surface aggregation or pore occlusion at the surface. Consequently, there is an expectation of enabling deeper penetration into the initial caries lesion. Moreover, the acid attack process may dissolve the crystals, potentially releasing

ions that serve as a reservoir for the remineralization of partially demineralized enamel. As a result, the groups treated with of nano-strontium/fluoride hydroxyapatite pastes exhibited the lesion depth reduction and increased mineral density. However, the 10%wt nano-strontium/fluoride hydroxyapatite group had a greater opportunity to form a protective layer or outer surface pore filling, increased crystallization in correlation with the concentration. This protective layer could inhibit the direct pore-filling into the subsurface lesion of artificial initial caries. As the result, the lesion depth regained in the 5%wt nano-strontium/fluoride hydroxyapatite group is better but with less opacity than the 10%wt nano-strontium/fluoride hydroxyapatite group. The results indicate that the lesion depth reduction achieved with the 5%wt nano-strontium/fluoride hydroxyapatite group is better, though it exhibits less opacity compared to the 10%wt nano-strontium/fluoride hydroxyapatite group. Nevertheless, no significant difference was observed when compared 5%wt to 10%wt nano-strontium/fluoride hydroxyapatite groups or between treatments lasting 7 and 14 days. Considering the material properties, the study suggests that 5%wt nano-strontium/fluoride hydroxyapatite is more beneficial for remineralization purposes.

In this study, EDS elemental line graphs and images revealed two remineralization patterns: top-down and bottom-up approaches. The sodium fluoride group showed the top-down remineralization pattern, while the nano-hydroxyapatite and nano-strontium/fluoride hydroxyapatite groups followed the bottom-up pattern. In the top-down approach, minerals are deposited from the enamel surface towards the deeper regions of the caries lesion. This pattern, which relies on ion-mediated crystal growth from the surrounding environment, typically results in less organized mineral deposition and non-uniform distribution.[32] Conversely, in the bottom-up pattern, mineral deposition starts from the deeper regions of the caries lesion and progresses towards the enamel surface. This method depends on particle-mediated nano-precursors, where nanoparticles penetrate the deeper sections of the carious lesion, leading to homogeneous mineral deposition and more uniform mineral distribution.[32] Moreover, as confirmed in EDS graphs, the pattern of nano-precursor deposition in the nano-strontium/fluoride hydroxyapatite groups presented more intensity and homogeneity than the 10%wt nano-hydroxyapatite group and 1500 ppm sodium fluoride group. It's important to note that neither fluorine from the sodium fluoride group nor strontium and fluorine from the nano-strontium/fluoride hydroxyapatite groups were detected in EDS graphs. This observation emphasizes the idea that nano-strontium/fluoride hydroxyapatite infiltrated the deeper parts of the caries lesion to fill the micropores, subsequently gradually releasing ions, serving as a reservoir that facilitates deep lesion remineralization. Using 1500 ppm sodium fluoride as a positive control, due to its well-established efficacy in remineralizing early demineralized enamel[8], it's worth noting that nano-hydroxyapatite also demonstrates a remineralizing effect comparable to that of sodium fluoride.[4,15,16,21,22] However, the enamel early lesions treated with nano-strontium/fluoride hydroxyapatite exhibited a statistically significant reduction in lesion depth compared to both sodium fluoride and nano-hydroxyapatite treatments. Although there was a better reduction in mineral loss with nano-strontium/fluoride hydroxyapatite, the difference was not statistically significant. Nano-strontium/fluoride hydroxyapatite may operate via two primary mechanisms that can be summarized as micropore filling and ions releasing. The rod-like nano-strontium/fluoride hydroxyapatite crystals fill the enamel micropores, replacing lost minerals of the partially demineralized enamel. Moreover, when exposed to acidic conditions often present in the oral environment, these crystals dissolve and release ions that aid remineralization. This suggests that nano-strontium/fluoride hydroxyapatite, with its rod-shaped crystal morphology, enhances remineralization efficiency and provides a more structured remineralization process. Essentially, it can replenish minerals from deep layers to the enamel surface while also leveraging ions to restore enamel minerals.

While the *in vitro* findings of this study are encouraging, the true validation will come from clinical trials and applications. Further clinical investigations are essential to validate these results and explore the long-term efficacy of nano-strontium/fluoride hydroxyapatite. As our study sourced the product from a single supplier, future research should aim to compare its effectiveness against other available dental products. Such comprehensive evaluations will establish the foundation for its incorporation into routine dental practice. The potential for nano-strontium/fluoride hydroxyapatite to revolutionize

the non-invasive treatment of early enamel caries is evident. Lastly, our findings suggest significant implications for clinical practice. The adoption of nano-strontium/fluoride hydroxyapatite might offer an effective, non-invasive strategy for managing early enamel caries. Nevertheless, before this treatment becomes a mainstay in dental practice, the practical considerations, including cost, feasibility, patient acceptance, and any associated risks, should be thoroughly assessed through extensive clinical trials.

## Conclusions

The use of nano-strontium/fluoride hydroxyapatite paste under the pH-cycling model for 7 days demonstrated superior remineralization capabilities on initial caries lesions when compared to 1500 ppm fluoride paste and nHA. Both 5%wt and 10%wt concentrations of nano-strontium/fluoride hydroxyapatite pastes yielded remineralization outcomes of comparable efficacy. The remineralization assessments measured lesion depth and mineral profile using micro-CT, as well as element analysis using SEM/EDS.

## Acknowledgments

The authors extend heartfelt gratitude to the Faculty of Dentistry at Prince of Songkla University, particularly for their indispensable expertise in micro-CT scanning. We also wish to acknowledge the significant contributions of the Faculty of Dentistry at Chulalongkorn University in conducting the SEM/EDS analysis. Nano-hydroxyapatite was provided from nanoX-im from Fluidinova, S.A., Moreira da Maia, Portugal. Special thanks are reserved for Assoc. Prof. Dr. Sirirat Tubsungnoen Rattanachan and Dr. Oranich Thongsri from Suranaree University of Technology for providing the experimental nano-strontium/fluoride hydroxyapatite and to Inno-age Laboratory for the experimental pastes preparation to this research.

## Conflicts of Interest

The remineralizing agents used in this study were provided by Inno-age Laboratory. The authors declare that there was no financial support or personal relationships that could have appeared to influence the work reported in this paper.

## References

1. Buzalaf MAR, Pessan JP, Honório HM, Ten Cate JM. Mechanisms of action of fluoride for caries control. Monogr Oral Sci. 2011;22:97-114.
2. Sadıkoğlu IS. White spot lesions: recent detection and treatment methods. Cyprus J Med Sci. 2020;5(3):260-6.
3. Frencken JE. Atraumatic restorative treatment and minimal intervention dentistry. Br Dent J. 2017;223(3):183-9.
4. Geeta R, Vallabhaneni S, Fatima K. Comparative evaluation of remineralization potential of nanohydroxyapatite crystals, bioactive glass, casein phosphopeptide-amorphous calcium phosphate, and fluoride on initial enamel lesion (scanning electron microscope analysis) – an *in vitro* study. J Conserv Dent. 2020;23(3):275-9.
5. Hicks J, Garcia-Godoy F, Flaitz C. Biological factors in dental caries: role of saliva and dental plaque in the dynamic process of demineralization and remineralization (part1). J Clin Pediatr Dent. 2003;28(1):47-52.
6. Robinson C, Shore R, Brookes S, Strafford S, Wood S, Kirkham J. The chemistry of enamel caries. Crit Rev Oral Biol Med. 2000;11(4):481-95.
7. Arifa MK, Ephraim R, Rajamani T. Recent advances in dental hard tissue remineralization: a review of literature. Int J Clin Pediatr Dent. 2019;12(2):139-44.
8. Walsh T, Worthington HV, Glenny AM, Marinho VC, Jeroncic A. Fluoride toothpastes of different concentrations for preventing dental caries. Cochrane Database Syst Rev. 2019;3(3):CD007868.
9. Featherstone JD. Dental caries: a dynamic disease process. Aust Dent J. 2008;53(3):286-91.
10. Featherstone JD. Prevention and reversal of dental caries: role of low level fluoride. Community Dent Oral Epidemiol. 1999;27:31-40.
11. Robinson C. Fluoride and the caries lesion: interactions and mechanism of action. Eur Arch Paediatr Dent. 2009;10(3):136-40.
12. Koo H. Strategies to enhance the biological effects of fluoride on dental biofilms. Adv Dent Res. 2008;20:17-21.
13. Aoun A, Darwiche F, Hayek SA, Doumit J. The fluoride debate: the pros and cons of fluoridation. Prev Nutr Food Sci. 2018;23:171-80.
14. Martínez-Mier EA. Fluoride: its metabolism, toxicity, and role in dental health. J Evid Based Complementary Altern Med. 2012;17:28-32.
15. Hannig M, Hannig C. Nanomaterials in preventive dentistry. Nat Nanotechnol. 2010;5:565-9.
16. Hannig M, Hannig C. Nanotechnology and its role in caries therapy. Adv Dent Res. 2012;24(2):53-7.
17. Balhuc S, Campian R, Labunet A, Negucioiu M, Buduru S, Kui A. Dental applications of systems based on hydroxyapatite nanoparticles—an evidence-based update. Crystals. 2021;11(6):674.

18. Bordea IR, Candrea S, Alexescu GT, Bran S, Băciuț M, Băciuț G, *et al*. Nano-hydroxyapatite use in dentistry: a systematic review. Drug Metab Rev. 2020;52(2):319-32.
19. Huang S, Gao S, Cheng L, Yu H. Remineralization potential of nano-hydroxyapatite on initial enamel lesions: an *in vitro* study. Caries Res. 2011;45(5):460-8.
20. Li L, Pan H, Tao J, Xu X, Mao C, Gub X, *et al.* Repair of enamel by using hydroxyapatite nanoparticles as the building blocks. J Mater Chem. 2008;18(34):4079-84.
21. Bossù M, Saccucci M, Salucci A, Giorgio GD, Bruni E, Uccelletti D, *et al.* Enamel remineralization and repair results of biomimetic hydroxyapatite toothpaste on deciduous teeth: an effective option to fluoride toothpaste. J Nanobiotechnology. 2019;17(1):17.
22. Juntavee A, Juntavee N, Hirunmoon P. Remineralization potential of nanohydroxyapatite toothpaste compared with tricalcium phosphate and fluoride toothpaste on artificial carious lesions. Int J Dent. 2021;2021(9):1-14.
23. Huang SB, Gao SS, Yu HY. Effect of nano-hydroxyapatite concentration on remineralization of initial enamel lesion *in vitro*. Biomed Mater. 2009;4(3):034104.
24. Wang L, Guan X, Yin H, Moradian-Oldak J, Nancollas GH. Mimicking the self-organized microstructure of tooth enamel. J Phys Chem C Nanomater Interfaces. 2008;112(15):5892-9.
25. Tabassum S. Role of substitution in bioceramics. In: Khan AS, Chaudhry AA, editors. Handbook of ionic substituted hydroxyapatites. Cambridge: Woodhead Publishing; 2020. p. 117-48.
26. Moloodi A, Toraby H, Kahrobaee S, Razavi MK, Salehi A. Evaluation of fluorohydroxyapatite/strontium coating on titanium implants fabricated by hydrothermal treatment. Prog Biomater. 2021;10:185-94.
27. Wang Q, Li P, Tang P, Ge X, Ren F, Zhao C, *et al.* Experimental and simulation studies of strontium/fluoride-codoped hydroxyapatite nanoparticles with osteogenic and antibacterial activities. Colloids Surf B Biointerfaces. 2019;182:110359.
28. Vacharangkura A, Kunawarote S, editors. Effects of experimental nano-hydroxyapatite pastes on remineralization of early demineralized enamel 2021: Rangsit University.
29. Arends J, ten-Bosch J. Demineralization and remineralization evaluation techniques. J Dent Res. 1992;71:924-8.
30. Theuns HM, van Dijk JW, Driessens FC, Groeneveld A. The effect of undissociated acetic-acid concentration of buffer solutions on artificial caries-like lesion formation in human tooth enamel. Arch Oral Biol. 1984;29(10):759-63.
31. Huang LH, Sun XY, Ouyang JM. Shape-dependent toxicity and mineralization of hydroxyapatite nanoparticles in A7R5 aortic smooth muscle cells. Sci Rep. 2019;9(1):18979.
32. Liu Y, Mai S, Li N, Yiu CKY, Mao J, Pashley DH, *et al*. Differences between top-down and bottom-up approaches in mineralizing thick, partially demineralized collagen scaffolds. Acta Biomater. 2011;7(4):1742-51.